*Human Molecular Genetics*, 2015, Vol. 24, No. 22 6485–6491

**doi: 10.1093/hmg/ddv357**
Advance Access Publication Date: 10 September 2015
Original Article

ORIGINAL ARTICLE

# *CDC174*, a novel component of the exon junction complex whose mutation underlies a syndrome of hypotonia and psychomotor developmental delay

Michael Volodarsky[1], Hava Lichtig[2], Tom Leibson[3], Yair Sadaka[3,4], Rotem Kadir[1], Yonatan Perez[1], Keren Liani-Leibson[1], Libe Gradstein[7], Ruthy Shaco-Levy[5], Zamir Shorer[3,4,8], Dale Frank[2] and Ohad S. Birk[1,6,*]

[1]The Morris Kahn Laboratory of Human Genetics, National Institute for Biotechnology in the Negev and Faculty of Health Sciences, Ben Gurion University, Beer Sheva 84105, Israel, [2]Department of Biochemistry, The Rappaport Family Institute for Research in the Medical Sciences, Faculty of Medicine, Technion, Israel Institute of Technology, Haifa 31096, Israel, [3]Department of Pediatrics, [4]Pediatric Neurology Unit, [5]Department of Pathology and, [6]Genetics Institute, Soroka University Medical Center, Ben Gurion University, Beer Sheva 84101, Israel, [7]Department of Ophthalmology, Soroka University Medical Center and Clalit Health Services, Ben Gurion University, Beer Sheva 84101, Israel and [8]Zlotowski Center of Neuroscience, Ben-Gurion University of the Negev, Beer Sheva 94105, Israel

*To whom correspondence should be addressed at: Genetics Institute, Soroka Medical Center, POB 151 Beer Sheva 84101, Israel. Tel: +972 8 6403439; Fax: +972 8 6400042; Email: obirk@bgu.ac.il



## Abstract

Siblings of non-consanguineous Jewish-Ethiopian ancestry presented with congenital axial hypotonia, weakness of the abducens nerve, psychomotor developmental delay with brain ventriculomegaly, variable thinning of corpus callosum and cardiac septal defects. Homozygosity mapping identified a single disease-associated locus of 3.5 Mb on chromosome 3. Studies of a Bedouin consanguineous kindred affected with a similar recessive phenotype identified a single disease-associated 18 Mb homozygosity locus encompassing the entire 3.5 Mb locus. Whole exome sequencing demonstrated only two homozygous mutations within a shared identical haplotype of 0.6 Mb, common to both Bedouin and Ethiopian affected individuals, suggesting an ancient common founder. Only one of the mutations segregated as expected in both kindreds and was not found in Bedouin and Jewish-Ethiopian controls: c.1404A>G, p.[*468Trpext*6] in *CCDC174*. We showed that CCDC174 is ubiquitous, restricted to the cell nucleus and co-localized with EIF4A3. In fact, yeast-two-hybrid assay demonstrated interaction of CCDC174 with EIF4A3, a component of exon junction complex. Knockdown of the *CCDC174* ortholog in *Xenopus laevis* embryos resulted in poor neural fold closure at the neurula stage with later embryonic lethality. Knockdown embryos exhibited a sharp reduction in expression of *n-tubulin*, a marker for differentiating primary neurons, and of hindbrain markers *krox20* and *hoxb3*. The *Xenopus* phenotype could be rescued by the human normal, yet not the mutant *CCDC174* transcripts. Moreover, overexpression of mutant but not normal CCDC174 in neuroblastoma cells caused rapid apoptosis. In line with the hypotonia phenotype, the *CCDC174* mutation caused depletion of RYR1 and marked myopathic changes in skeletal muscle of affected individuals.

**Received:** May 15, 2015. **Revised:** August 2, 2015. **Accepted:** September 1, 2015

## Introduction

Two siblings of non-consanguineous Jewish-Ethiopian kindred (Fig. 1A, P1) presented with a syndrome of congenital myopathy and psychomotor developmental delay: both were born at term, following normal pregnancies. Severe hypotonia of limbs and trunk was evident at birth, requiring ventilation as of 1 month of age and feeding through gastrostomy. Strabismus, with bilateral weakness of the abducens nerve, was evident, as were elongated face and open mouth reflecting low muscle tone. Undescended testes were found in the male and a small cardiac ventricular septal defect (VSD) in both siblings. No specific dysmorphism was seen. Mild psychomotor retardation, both gross and fine motor, was evident as was delay in speech acquisition. Blood creatine phosphokinase (CPK), lactate, ammonia, selenoprotein and amino acids, as well as urinary organic acids, were within normal limits. Karyotype, chromosomal microarray as well as molecular testing for *DMPK* mutations (myotonic dystrophy), Duchenne muscular dystrophy, Prader Willi and spinomuscular atrophy (SMA) were normal. Nerve conduction velocity testing was non-conclusive, suggesting a myopathy or a disease of the neuromuscular junction (NMJ). Single-fiber electromyography (SFEMG) suggested a myopathy or an NMJ defect as in myasthenia, yet tensilon testing was negative. Brain magnetic resonance imaging (MRI) at the age of 1 year demonstrated dilated lateral ventricles and thinning of corpus callosum with hypoplasia of uvula nodule vermis. Spinal cord MRI was normal. Growth in terms of height, weight and head circumference was normal. Muscle biopsy findings demonstrated random variability of muscle fiber size with no evidence of necrosis, no enhancement of endomesial fibrotic tissue or immune cell infiltrates. Immunohistochemistry staining for myosin demonstrated relative abundance of type 1 fibers. There was no evidence of glycogen storage or mitochondrial dysfunction. Staining for cox, desmin, spectrin, sarcoglycans (α, β, γ, δ), merosin (80 and 300 kD) and dystrophin 1–3 were normal. Electron microscopy (EM) studies demonstrated destruction of myofibrils with no evidence of regeneration or inflammation or glycogen storage (data not shown). Within the differential diagnosis, a possibility of merosin-positive muscular dystrophy was raised.

A similar phenotype was observed in four affected individuals of a consanguineous Israeli Arab Bedouin kindred (Fig. 1A, P2). All four were born at term following uneventful pregnancies (reduced fetal movements were suggested in retrospect by the mother in some of the pregnancies). Severe axial hypotonia, psychomotor developmental delay (gross and fine motor) and weakness/palsy of the abducens nerve were evident. All four had undescended testes and cardiac VSD or atrial septal defects (ASD). Blood CPK, lactate, ammonia, amino acids, very long fatty acids, as well as urinary organic acids, were within normal limits. Molecular testing for SMA was normal. Nerve conduction velocity studies showed normal distal latencies, amplitudes and velocities of the examined nerves, while electromyography (EMG) demonstrated small sharp units, suggesting possible myopathy. There was no improvement with neostigmine. Brain MRI was done for two of the individuals at 2 months of age, demonstrating no significant structural abnormalities. All four patients underwent skeletal muscle biopsy and showed myopathic changes of moderate to severe degree. Endomysial and perimysial fibrosis with replacement of muscle fibers by fibrous tissue was evident. Increased variation in fiber size was seen in all biopsies, with small atrophic fibers, some normal-sized and scattered large hypertrophic fibers. Sporadic fibers with internal nuclei were observed [Fig. 2D, patient P2-IV1 (Fig. 1A)]. All biopsies showed no evidence of fiber grouping (ruling out neurogenic myopathy). In addition, no mitochondrial aggregates were identified, and there was no evidence of accumulation of lipid or glycogen. All biopsies were immunoreactive with dystrophin 1–3, spectrin and merosin. While three of the Bedouin patients died by the age of 4 months (one is still alive at 2 years of age), both Ethiopian patients are still alive at the ages of 8 and 9 years, though on continuous positive airway pressure (CPAP) and gastrostomy feeding. We set out to identify the molecular basis of the similar phenotypes in both kindreds of completely different ancestral origins.

## Results

### Linkage analysis and identification of the disease-associated mutation

As the parents of the Jewish-Ethiopian siblings were non-consanguineous (tracing at least seven generations back) yet of the same ethnic origins and inbred community, we assumed possible homozygosity of a founder mutation in the affected children. Affymetrix 250 K single nucleotide polymorphism (SNP) arrays, testing all four family members, identified a single 3.5 Mb homozygosity locus on chromosome 3 (Fig. 1B) that was shared by both affected individuals (Fig. 1A, P1:II-1 and P1:II-2). Whole exome sequence analysis of the affected male identified within the 3.5 Mb locus only three homozygous mutations: in *NUP210*, *GRIP2* and *CCDC174* (*C3orf19*), encoding coiled-coil domain containing 174. The mutations were verified through Sanger sequencing (not shown). Illumina 6 K array analysis done for all four affected individuals in the Bedouin kindred and their parents as well as Affymetrix 250 K analysis done for individual P2:IV-6 (Fig. 1A), identified a single 18 Mb homozygosity locus that was shared by all affected individuals (Fig. 1B). Fine mapping using polymorphic markers within the 18 Mb locus, testing all available family members, narrowed the locus down to 13 Mb on chromosome 3, encompassing the entire 3.5 Mb locus of the Ethiopian family (Fig. 1A, P2 and B).

While *GRIP2* and *CCDC174* were within the locus shared by both families, *NUP210* was not. Whole exome sequencing done for individual P2-IV:6 (Fig. 1A, P2) identified within the entire 13 Mb locus only two homozygous mutations: the same *GRIP2* and *CCDC174* mutations that were found in the Ethiopian family. Testing the available individuals of the Bedouin kindred for the *GRIP2* mutation through Sanger sequencing identified a healthy individual (Fig. 1A, P2-IV:2) who was homozygous for the mutation. Thus, the only mutation common and unique to the affected individuals of both kindreds was c.1404A>G, p.(*468Trpext*6) in *CCDC174*, NM_016474.4(CCDC174_v001), termed also *c3orf19* (Fig. 1C). The stop codon loss mutation is predicted to extend the CCDC174 protein by six additional amino acids. Restriction analysis for the *CCDC174* mutation demonstrated full segregation within the entire tested kindred. The *CCDC174* mutation was not found in 400 Bedouin non-related controls, while one carrier was found among 100 available Jewish-Ethiopian non-related controls. Interestingly, within the overlapping 0.6 Mb, the affected Ethiopian and Bedouin individuals were shown to have identical haplotypes, as evidenced by the 39 SNPs (Fig. 1B; Supplementary Material, Fig. S1) and two mutations within the shared locus.

### Characterization of *CCDC174*

As there was no published information regarding *CCDC174*, we initiated its characterization: human *CCDC174* is ubiquitously

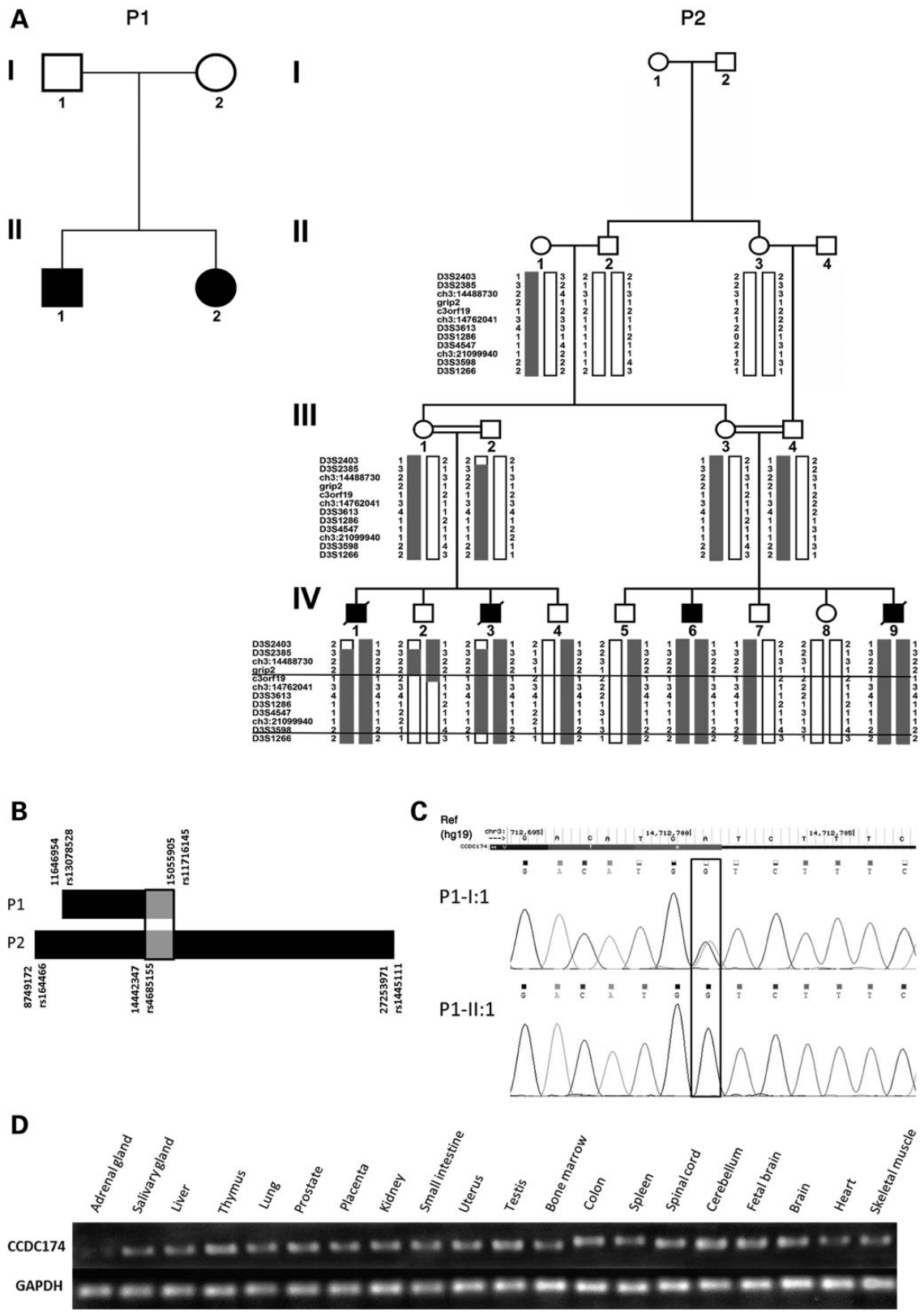


**Figure 1.** Pedigrees of studied kindred and the *CCDC174* mutation: (**A**) the affected Jewish-Ethiopian kindred (P1) and the affected Bedouin kindred (P2). Fine mapping demonstrates the disease-associated chromosome 3 locus. (**B**) Homozygosity at the shared locus. Black rectangles represent the homozygosity blocks per each pedigree. Gray is the identical haplotype shared by both P1 and P2. Physical positions (chromosome 3) and SNP rs IDs are given. (**C**) Sequence analysis demonstrating the *CCDC174* mutation. Reference sequence from UCSC genome browser. Heterozygosity for the wild-type and the mutant allele and homozygosity for the mutant allele (black frame) in obligatory carrier and affected individual, respectively. (**D**) *CCDC174* is ubiquitously expressed. PCR and electrophoresis of human cDNA panel. *GAPDH* expression was used as control.

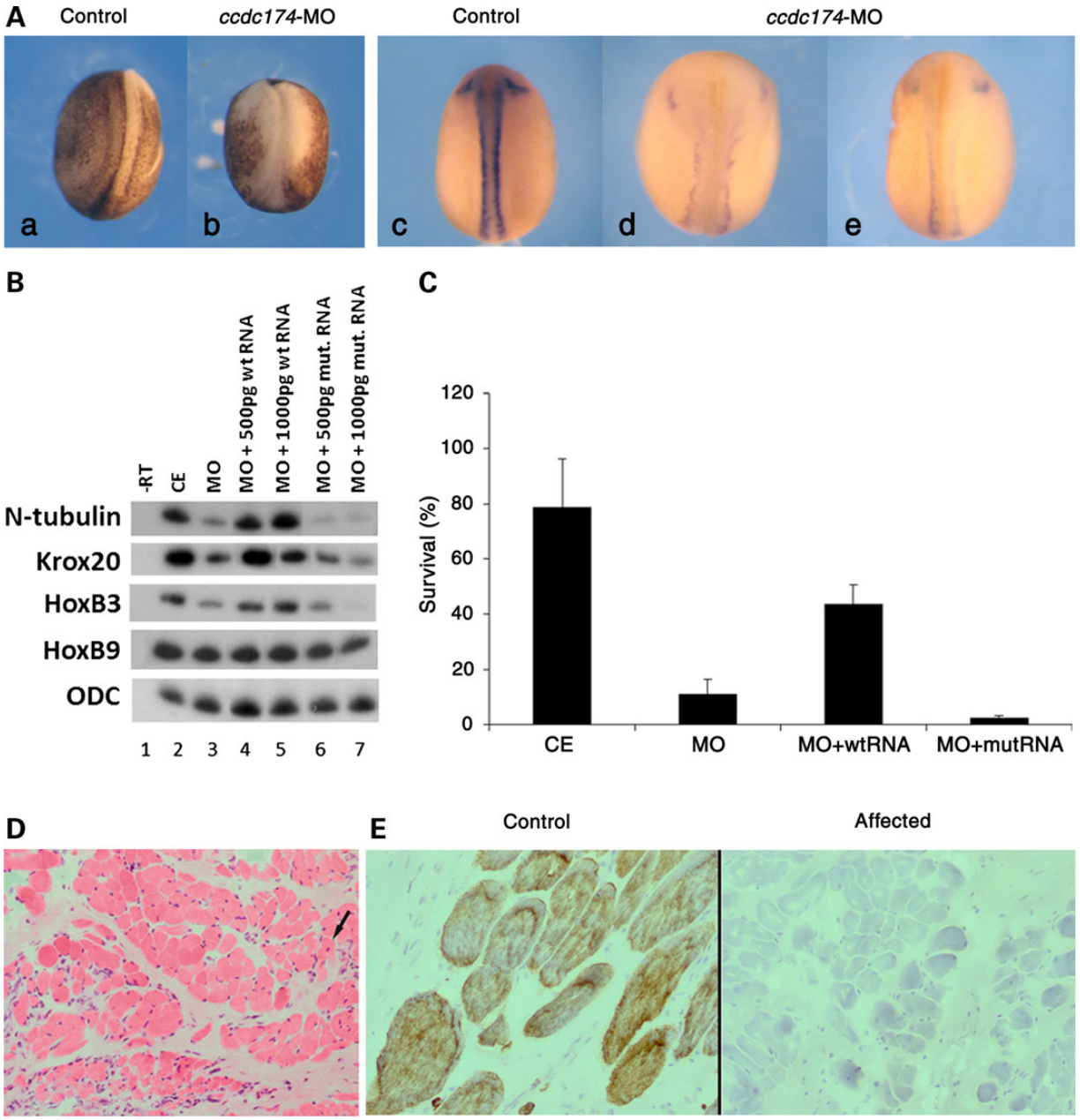


**Figure 2.** CCDC174 protein knockdown in *Xenopus* embryos reduces neural folding and expression of neural markers and affects embryonic survival. (**A**) Neural folding and primary neuron marker expression. (a) In control embryos, normal neural folds were observed in 98% of the neurula stage embryos ($n = 40$). (b) In embryos injected with the *CCDC174*-MO (9 ng), an open neural folds phenotype was observed in 96% of the neurula stage embryos ($n = 52$), only 4% of the embryos had normal neural folding, like their siblings in (a). One representative embryo is shown for control and *CCDC174*-MO with a typical neural plate phenotype. (c) Whole-mount *in situ* hybridization to the *n-tub* marker of primary neuron differentiation in the uninjected control group; *n-tub* is expressed at normal levels in 88% of the embryos ($n = 16$). (d and e) Whole-mount *in situ* hybridization to the *n-tub* marker in embryos injected at the one-cell stage with *CCDC174*-MO (9 ng). *n-tub* expression levels are reduced in in 93% of the embryos ($n = 14$). One representative embryo is shown for control and two representative embryos for *CCDC174*-MO. Note the more open neural plates in (d and e) versus (c). (**B**) CCDC174 protein knockdown reduces the expression of neural markers. Embryos were injected at one-cell stage with *CCDC174*-MO (9 ng) alone (Lane 3) or together with RNA (500 or 1000 pg) encoding the wild-type or mutant human ccdc174 proteins (Lanes 4–7). Total RNA was isolated from pools of seven embryos at neurula stage. Expression of the following neural marker genes was examined by sqRT-PCR: *n-tub*, *krox20*, *hoxb3* and *hoxb9*. *Odc* serves as a control for RNA levels in each sample. RT-PCR was performed on RNA isolated from control embryos (Lane 1). sqRT-PCR analysis of RNA isolated from uninjected control embryos (CE) serves as a positive control (Lane 2). (**C**) CCDC174 protein knockdown affects embryonic survival. Embryos injected at the one-cell stage with the *CCDC174*-MO (9 ng) alone ($n = 199$) or together with RNA (1000 pg) encoding wild-type ($n = 194$) or mutant ($n = 134$) human CCDC174 protein were scored at the tailbud stage for survival, in comparison with uninjected control embryos ($n = 162$). The bars represent the percentage of embryos surviving from neurula to tailbud stages in three independent experiments. (**D**) Myopathic changes represented by replacement of muscle fibers by fibrous tissue, marked variation in fiber size and rare fibers with internal nuclei (arrow) (hematoxylin & eosin, original magnification ×200). (**E**) Immunohistochemical staining of muscle biopsy sections with anti-RYR1 antibody. Duchenne muscular dystrophy biopsy served as control (original magnification ×200).

expressed (Fig. 1D). CCDC174 protein as well as its C-terminal end and stop codon are highly conserved among vertebrates (UCSC vertebrate Mulitz alignment and conservation browser, integrating phastCons and phyloP).

To better understand the functional significance of *CCDC174* and the impact of the mutation found, we studied its *Xenopus* ortholog, *ccdc174*. At neurula stages, *ccdc174*-MO injected embryos exhibited poor neural folds closure versus uninjected controls (Fig. 2A, a and b). By whole-mount *in situ* hybridization, these same embryos with poor neural folding also had a sharp reduction in *n-tubulin* (*n-tub*) gene expression (Fig. 2A, c and e); *n-tub* is a marker for differentiating primary neurons. Pools of *ccdc174* morphant versus control embryos were examined by semi-quantitative reverse transcription PCR (sqRT-PCR) for expression of additional neural markers (Fig. 2B). In *ccdc174* knockdown embryos, there was also a strong reduction in hindbrain marker (*krox20* and *hoxb3*) gene expression (Fig. 2B, Lanes 2 and 3). In contrast, spinal cord (*hoxb9*) and neural crest (not shown) marker gene expression was not significantly modulated (Fig. 2B, Lanes 2 and 3). These results show that some aspect of early neural plate patterning and neuron formation is disrupted by ccdc174 protein knockdown. The *ccdc174* morphant embryos had neural folds defects but were still alive at neurula stages. However, by later tailbud stages, survival was only 10%, reduced 8-fold versus control embryos (Fig. 2C). Thus, the *ccdc174* knockdown phenotype in *Xenopus* is embryonic lethal at later stages.

## Functional studies of the human *CCDC174* mutation

To assay function of wild-type versus mutant human CCDC174 protein in *Xenopus* embryos, *in vitro* transcribed mRNAs encoding these proteins were separately injected into *ccdc174*-MO embryos. Ectopic expression of the wild-type human CCDC174 protein rescued the *ccdc174*-MO phenotype, leading to an increased control-like expression of the *n-tub*, *krox20* and *hoxb3* genes (Fig. 2B, Lanes 2–5). Unlike the wild-type protein, the mutant protein did not rescue neural marker expression (Fig. 2B, Lanes 2 and 3, 6 and 7). Moreover, the mutant human CCDC174 appeared to slightly enhance the inhibited expression of neural genes, even more than in the *ccdc174*-MO group alone (Fig. 2B, Lanes 3, 6 and 7).

Sharp differences in rescue were detected between the wild-type and mutant human CCDC174 proteins in the survival assay. In wild-type CCDC174/*ccdc174*-MO co-injected tailbud stage embryos, survival was highly enhanced, increasing over 4-fold versus the *ccdc174*-MO group (Fig. 2C). However, in the mutant CCDC174/*ccdc174*-MO co-injected embryos, survival was almost 3-fold lower than in the *ccdc174*-MO group, and over 10-fold lower than the wild-type rescued group (Fig. 2C). This result shows that unlike the wild-type protein, the mutant CCDC174 protein does not functionally replace endogenous *Xenopus* ccdc174 protein. Ectopic expression of either normal or mutant CCDC174 protein into normal embryos expressing endogenous *Xenopus* ccdc174 protein gave no significant phenotypes (not shown).

## Interaction of wild-type and mutant *CCDC174* with *EIF4A3*

Possible interaction between CCDC174 and EIF4A3 was previously suggested based on a massive protein–protein interaction screen (1). EIF4A3 is a core component of the exon junction complex (EJC), which plays a critical role in processing of RNA, nonsense-mediated decay and translation (2). To get further insight regarding the CCDC174-EIF4A3 interaction and the effect of the *468Trpext*6 mutation, we performed transfections of EIF4A3, CCDC174-WT and CCDC174-MUT expression vectors into a neuroblastoma cell line. Transfection of EIF4A3 and CCDC174-WT separately showed that both proteins are nuclear (Fig. 3A, a and b, respectively). While some cells showed also cytosolic EIF4A3 (not shown), CCDC174 was exclusively restricted to the nucleus. Co-transfection of EIF4A3 with either normal or mutant

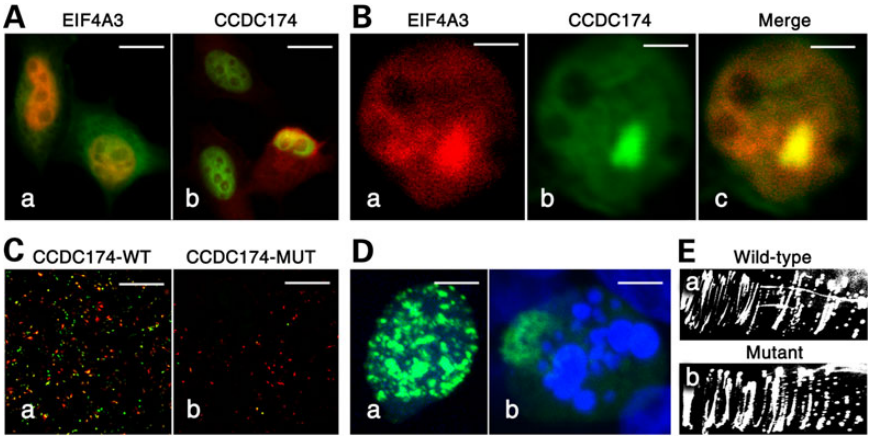


**Figure 3.** *In vitro* studies of CCDC174-EIF4A3 interactions and the CCDC174 mutation effect in neuroblastoma cells. (**A**) CCDC174 and EIF4A3 are nuclear proteins. Confocal microscopy showing intracellular localization of EIF4A3 (a) and wild-type CCDC174 (b) in the nucleus of neuroblastoma cells transfected with both constructs. EIF4A3 was fused to RFP, while wild-type or mutant CCDC174 was fused to GFP (pEGFP-C2 expression vector). Co-transfection of an empty vector expressing a different fluorescent marker was performed for transfection internal control and background cytosolic fluorescence. Scale bar 15 µm. (**B**) CCDC174 and EIF4A3 are co-localized. Confocal microscopy showing a nucleus of a single cell transfected with both EIF4A3 (a) and wild-type CCDC174 (b). Marked co-localization of both proteins is shown in the merged image (c). Co-localization of EIF4A3 and the mutant CCDC174 was also evident (not shown); scale bar 5 µm. (**C**) Overexpression of the mutant CCDC174 in neuroblastoma cells induces apoptosis. Confocal microscopy showing overexpression of CCDC174-WT (a) or CCDC174-MUT (b). Both photos were taken 24 h post-transfection of vectors to a similar number of cells. Co-transfection of an empty vector expressing RFP was performed as an internal control; scale bar 340 µm. (**D**) Mutant CCDC174 aggregates and causes fragmentation of genomic DNA. Confocal microscopy of neuroblastoma cells overexpressing mutant CCDC174, showing aggregation of mutant CCDC174 in the nucleus (a); scale bar 9 µm. DNA fragmentation of apoptotic CCDC174-MUT-transfected cell can be seen following 4′,6-diamidino-2-phenylindole staining (b); scale bar 4 µm. (**E**) Both wild-type and mutant CCDC174 interact with EIF4A3. Yeast-two-hybrid assay showing interaction between EIF4A3 and normal (a) but also mutant (b) CCDC174. Yeast colonies appeared 48 h after plating on a selective medium, indicating a strong protein–protein interaction.

CCDC174 showed marked co-localization in the nucleus (Fig. 3B). This was further validated by yeast-two-hybrid assay, which showed interaction of EIF4A3 with both wild-type and mutant CCDC174 protein (Fig. 3E, a and b, respectively; Supplementary Material, Fig. S2). Interestingly, overexpression of the mutant (CCDC174-MUT) but not the normal (CCDC174-WT) protein resulted in rapid and massive apoptosis of cells (Fig. 3C, b and a, respectively; Fig. 3D, b) while aggregation of CCDC174-MUT in the nucleus was evident (Fig. 3D, a).

### Effect of the *CCDC174* mutation on RYR1

Knockdown of *eif4a3* in *Xenopus* results in full-body paralysis of embryos due to downregulation and improper splicing at the 3′ end of *ryr1* transcripts (3). To evaluate the effect of the CCDC174 mutation on RYR1, we used anti-RYR1 antibody for immunohistochemical staining of muscle biopsy sections derived from an affected individual (Fig. 1A, P2-IV6). While cytoplasmic immunoreactivity was clearly evident in the control case, no immunoreactivity was observed in the case biopsy (Fig. 2E).

## Discussion

We demonstrated that CCDC174 is a ubiquitously expressed nuclear protein. It interacts with EIF4A3, as demonstrated both through yeast-two-hybrid data and through co-localization experiments in neuroblastoma cells. Thus, CCDC174 is part of the EJC, some of whose components have been shown to take part in neuron-related processes such as neural stem cell division (4), as well as impacting synaptic plasticity and behavior (5). Moreover, mutations in EJC genes have been shown to cause mental retardation as well as behavior and muscular phenotypes (3–5).

The human and *Xenopus* data put together demonstrate that *CCDC174* is essential for neuronal differentiation and that its founder mutation, common to a Jewish-Ethiopian family and a Bedouin kindred, underlies a severe autosomal recessive syndrome of hypotonia, psychomotor developmental delay and abducens nerve palsy. The *CCDC174* mutation found in the patients does not affect the nuclear localization of the protein or its interaction with EIF4A3. When overexpressed in neuroblastoma cells, the mutated protein does, however, cause apoptosis of neuroblastoma cells *in vitro*, preceded by formation of mutant CCDC174 nuclear aggregates.

In the *Xenopus* experiments, while the wild-type human CCDC174 rescued the *ccdc174*-silencing phenotype, the mutant CCDC174 not only failed to rescue the silencing phenotype, but rather induced an even somewhat more severe phenotype as demonstrated in the survival rates (Fig. 2C). This enhanced severity of the *Xenopus* phenotype seen with the mutant CCDC174 could imply co-dominance or toxic gain of function, possibly due to unexpected interactions between massive amounts of the human mutant protein with endogenous *Xenopus* proteins. In line with the recessive heredity of the human disease, ectopic expression of either normal or mutant CCDC174 protein into normal embryos expressing endogenous *Xenopus* ccdc174 protein gave no significant phenotypes. Regarding the hypotonia phenotype of the affected individuals, we showed that no RYR1 could be detected in a muscle biopsy of an affected individual, in line with the downregulation of *ryr1* caused by *eif4a3* knockdown in *Xenopus*.

While the Ethiopian-Jewish community is inbred, consanguineous marriages have been carefully avoided, with a tradition of verifying lack of consanguinity seven generations back in every marriage. We have recently demonstrated that social structure of an inbred community can be deciphered through genomic data (6). Specifically, we showed that while genomic similarities due to recent intermarriages between social groups are reflected in shared large loci, common ‘old’ founder loci are reflected in sharing of small loci (6). The above is well demonstrated in that the founder mutation of the Ethiopian family lies within a single small 3.5 Mb locus of homozygosity in the entire genome.

Of unique interest is the fact that the mutation in the Jewish-Ethiopian family was found also in a Bedouin kindred, within a shared identical 0.6 Mb genomic segment. The origins of Israeli Bedouins are diverse (6), and the specific Bedouin kindred originates from Egypt. The Jewish-Ethiopian community has been shown to cluster with its neighboring autochthonous population in Ethiopia (7). Mitochondrial DNA studies of Egyptians of the Gurma region near Thebes, considered to be descendants of ancient Egyptians, demonstrated unique similarities specifically to the Ethiopian population (8). Thus, it is perhaps not surprising that the Bedouin-Egyptian and Jewish-Ethiopian families share an ancient founder mutation.

## Materials and Methods

### Genetic studies

SNP arrays were done as previously described (9). Whole exome sequencing was performed as previously described (9). After filtering for known variants (SNP database http://www.ncbi.nlm.nih.gov/projects/SNP, Seattle, WA, http://evs.gs.washington.edu/EVS, accessed December 2011), sequence variants that were not annotated in any of the database SNP or 1000 genomes databases were prioritized for further analysis. Variants identified within the disease-associated locus through whole exome sequencing were verified using Sanger sequencing. Analysis for the *CCDC174* mutation was done through polymerase chain reaction (PCR) (forward primer 5′AGCCCTGAACATACGTCACC3′; reverse 5′AATCCAACCCGAAGTCTGTG3′) followed by DpnII restriction (wild-type 109 and 135 bp fragments; mutant 244 bp fragment).

### Xenopus studies

*Xenopus* ovulation, *in vitro* fertilization, culture and staging were done as described (10). To knockdown *Xenopus* ccdc174 protein, one-cell stage embryos were injected with 9 ng of the translational blocking *ccdc174*-antisense translational blocking morpholino oligonucleotide (MO; Gene Tools). The *ccdc174*-MO sequence is 5′GCAGCTTCTTCTTCCTGTCCATTGT3′. In rescue experiments, capped *in vitro* transcribed RNAs (500–1000 pg) encoding either the wild-type or mutant human CCDC174 proteins were separately co-injected into the *ccdc174*-MO embryos. Embryos were cultured to neurula stages, and total RNA was isolated for semi-quantitative sqRT-PCR analysis (11). Expression of the following genes was examined by sqRT-PCR: *ODC* (housekeeping positive control for RNA loading), *n-tubulin* (*n-tub*—primary neuron marker), *krox20* and *hoxb3* (hindbrain markers) and *hoxb9* (spinal cord marker). Each experiment was repeated at least three times, and individual samples are typically assayed three times for each marker. Whole-mount *in situ* hybridization was performed (12) with the *n-tubulin* probe (13).

### *In vitro* studies

Constructs were generated for transient transfections: EIF4A3 was fused to RFP, while wild-type or mutant CCDC174 was

fused to GFP (pEGFP-C2 expression vector). Neuroblastoma cell line was cultured on glass coverslips to 50–60% confluence and transiently transfected with 1 μg DNA of either expression vector or both using lipofectamin2000 (Invitrogen) following the manufacturer's instructions. Transfected cells were examined under an Olympus Fluoview FV1000 confocal laser scanning microscope. Co-transfection of an empty vector expressing a different fluorescent marker was performed for transfection internal control and background cytosolic fluorescence. Yeast-two-hybrid assay was performed using the commercial GAL4-based Two-Hybrid Phagemid Vector Kit (Stratagene) following the manufacturer's instructions.

## Supplementary Material

Supplementary Material is available at *HMG* online.

*Conflict of Interest statement*. None declared.

## Funding

This work was supported by Teva Pharmaceutical Industries Ltd under the Israeli National Network of Excellence in Neuroscience (NNE) established by Teva; by the Legacy Heritage Bio-Medical Program of the Israel Science Foundation (Grant No. 1814/13); and through the Kahn Family Foundation. D.F. was supported by a grant from the Israel Science Foundation (658/09).

## References

1. Rual, J.F., Venkatesan, K., Hao, T., Hirozane-Kishikawa, T., Dricot, A., Li, N., Berriz, G.F., Gibbons, F.D., Dreze, M., Ayivi-Guedehoussou, N. *et al*. (2005) Towards a proteome-scale map of the human protein protein-protein interaction network. *Nature*, **437**, 1173–1178.
2. Haremaki, T., Sridharan, J., Dvora, S. and Weinstein, C.D. (2010) Regulation of vertebrate embryogenesis by the exon junction complex core component Eif4a3. *Dev. Dyn.*, **239**, 1977–1987.
3. Haremaki, T. and Weinstein, C.D. (2012) Eif4a3 is required for accurate splicing of the *Xenopus laevis* ryanodine receptor pre-mRNA. *Dev. Biol.*, **372**, 103–110.
4. Silver, D.L., Watkins-Chow, D.E., Schreck, K.C., Pierfelice, T.J., Larson, D.M., Burnetti, A.J., Liaw, H.J., Myung, K., Walsh, C.A., Gaiano, N. *et al*. (2010) The exon junction complex component Magoh controls brain size by regulating neural stem cell division. *Nat. Neurosci.*, **13**, 551–558.
5. Chuang, T.W., Lee, K.M. and Tarn, W.Y. (2015) Function and pathological implication of exon junction complex factor Y14. *Biomolecules*, **5**, 343–355.
6. Markus, B., Alshaffe, I. and Birk, O.S. (2014) Deciphering the fine structure of tribal admixture in the Bedouin population using genomic data. *Heredity*, **1121**, 182–189.
7. Behar, D.M., Yunusbayev, B., Metspalu, M., Metspalu, E., Rosset, S., Parik, J., Rootsi, S., Chaubey, G., Kutuev, I., Yudkovsky, G. *et al*. (2010) The genome-wide structure of the Jewish people. *Nature*, **466**, 238–242.
8. Kings, T., Salem, A.E., Bauer, K., Geisert, H., Malek, A.K., Chaix, L., Simon, C., Welsby, D., Di rienzo, A., Utermann, G. *et al*. (1999) mtDNA Analysis of Nile River Valley populations: a genetic corridor or a barrier to migration? *Am. J. Hum. Genet.*, **64**, 1116–1176.
9. Volodarsky, M., Markus, B., Cohen, I., Staretz-Chacham, O., Flusser, H., Shelef, I., Langer, Y. and Birk, O.S. (2013) A deletion mutation in TMEM38B associated with autosomal recessive osteogenesis imferfecta. *Hum. Mutat.*, **34**, 582–586.
10. Elkouby, Y.M., Polevoy, H., Gutkovich, Y.E., Michaelov, A. and Frank, D. (2012) A hindbrain-repressive Wnt3a/Meis3/Tsh1 circuit promotes neuronal differentiation and coordinates tissue maturation. *Development*, **139**, 1487–1497.
11. Gutkovich, Y.E., Ofir, R., Elkouby, Y.M., Dibner, C., Gefen, A., Elias, S. and Frank, D. (2010) Xenopus Meis3 protein lies at a nexus downstream to Zic1 and Pax3 proteins, regulating multiple cell-fates during early nervous system development. *Dev. Biol.*, **338**, 50–62.
12. Zetser, A., Frank, D. and Bengal, E. (2001) MAP kinase converts MyoD into an instructive muscle differentiation factor in Xenopus. *Dev. Biol.*, **240**, 168–181.
13. Fonar, Y., Gutkovich, Y.E., Root, H., Malyarova, A., Aamar, E., Golubovskaya, V.M., Elias, S., Elkouby, Y.M. and Frank, D. (2011) Focal adhesion kinase protein regulates Wnt3a gene expression to control cell fate specification in the developing neural plate. *Mol. Biol. Cell.*, **22**, 2409–2421.